ELSEVIER

Catalysis Today 39 (1997) 207–218

CATALYSIS TODAY

Quantitative studies on the heterogeneous gas-phase photooxidation of CO and simple VOCs by air over TiO_2

A.V. Vorontsov[a], E.N. Savinov[a], G.B. Barannik[a], V.N. Troitsky[b], V.N. Parmon[a,*]

[a]*Federal Research Centre, Boreskov Institute of Catalysis, Prospekt Akademia Lavrentieva 5, Novosibirsk 630090, Russian Federation*
[b]*Institute on New Chemical Problems, Chernogolovka, Moscow Region 142432, Russian Federation*

Abstract

This paper presents a collection of the authors' recent results concerning the photocatalytic oxidation of gaseous organics and CO over TiO_2 in different kinds of reactors with the accent on providing quantitative information about the photoprocesses studied to enable comparison with results of other authors. A static reactor, an annular flow reactor and a flow-circulating reactor were used. Oxidation of acetone, ethanol and diethyl ether in the static reactor ultimately leads to CO_2, with acetaldehyde, acetaldehyde and ethyl acetate being the intermediate products in the oxidation of ethanol and diethyl ether, respectively. Acetone is completely oxidized to CO_2 during a single pass through the annular flow reactor if the residence time is greater than 1 min. Temperature dependence of the acetone photooxidation rate in the flow-circulating reactor has a maximum at 80°C. Four specimens of TiO_2 prepared by principally different methods were tested in oxidation of acetone and CO in the flow-circulating reactor. It has been found that photoplatinization retards the acetone oxidation and prohibits considerably the CO oxidation. These results indicate that the process of heterogeneous photocatalytic oxidation can be substantially improved by optimization of both the catalyst and the conditions of the photocatalytic process. © 1997 Elsevier Science B.V.

Keywords:

1. Introduction

Volatile organic compounds (VOCs) together with nitrogen and sulfur oxides as well as carbon monoxide are the most widespread air pollutants. Heterogeneous photocatalytic oxidation over TiO_2 of these air contaminants is now widely recognized as a potential method for their destruction. The photocatalytic oxidation over TiO_2 in the gas phase has been demonstrated for alkanes [1–8], cyclohexane [9], propene [10], 1,3-butadiene [11], benzene [12], toluene [11,13,15], *m*-xylene [16], methanol [7], ethanol [14,17], isopropanol [7,18–22], butanols [16,22], methylbutanols [3,21], formaldehyde [11,16], acetaldehyde [13,14,23,25], propionaldehyde [24], butyraldehyde [16], acetone [16,26], isobutiric acid [13], pyridine [27], nitroglycerin [28], methyl mercaptane [13], trichloroethylene [29–37], and CO [1,38–40]. In all these cases CO_2 was the ultimate gaseous carbon-containing product; however, a large set of oxidation intermediates has also been detected, including hazardous ones. In this paper we report data on formation of intermediates during the photocatalytic oxidation of

*Corresponding author. Fax: 7-383 235 5766; e-mail: parmon@caty.catalysis.nsk.su

PII S0920-5861(97)00102-8

acetone, ethanol and diethyl ether over TiO_2 in a static system. Of vital significance for air decontamination in practice is to prevent these hazardous compounds from releasing.

Photocatalytic methods for air purification have a variety of merits, the main advantages being their ability to operate at mild and ambient conditions and to provide additionally a bactericidal action. The main disadvantage is a sufficiently low pollutants oxidation rate, in comparison with thermal catalytic oxidation, due to a low value of UV light flux. Therefore, the photocatalytic method for air purification should fit well for the next cases:

1. Continuous treatment of slow air flows containing appreciable concentration of pollutants.
2. Continuous treatment of fast air flows containing trace concentration of pollutants.
3. Continuous treatment of fast air flows containing pollutants with unstable concentrations that are appreciable only in short periods of time. During these short periods, the pollutants can adsorb on the photocatalyst surface and thereafter be oxidized, preparing, thus, the photocatalyst surface for the adsorption of the pollutants from the next pollutants pulse.

Each case demands that the photocatalytic reactor be of a different configuration. Case (1) is the simplest one and the smallest reactor can be used. Case (2) requires a reactor providing a good contact between the contaminated air flow and the illuminated photocatalyst. In addition to this, a reactor for case (3) has to contain the amount of photocatalyst sufficient to adsorb the whole of the pollutant containing in its pulse. In this paper we report some data on the acetone photocatalytic oxidation in an annular flow reactor for case (1).

The quantitative approach is the basis of modern science. This approach means to obtain as much quantitative information on a system under consideration as possible and reasonable. Nevertheless, one should avoid overobtaining quantitative data in order to be protected from supplying useless and/or unreliable information.

In catalysis, a quantitative study implies obtaining reliable information on the catalytic activity which should be best expressed as a turnover number, i.e., the number of molecules reacted on one active site per second. The turnover number is the best basis for comparison of the catalysts. However, since in the heterogeneous catalysis the number of active sites is only very seldom known, comparison is done usually on the basis of specific rates: the number of molecules reacted on unit of the catalyst surface area per second. Evidently, to compare adequately different catalysts, the reaction conditions that influence the reaction rate have to be identical.

As to photocatalysis, a basis for the comparison must take into account only illuminated parts of the catalyst. Since the most of active photocatalysts used in gas-phase reactions are powdered films, it is not easy to determine the surface of the illuminated parts. Two approaches can be used here: 'fundamental' and 'applied'. The former approach should provide specific rate,[1] i.e. the rate on unit of the illuminated catalyst surface area, either by rough estimation of the light penetration depth into the photocatalyst or using very thin translucent films. However, the thin film technique fails when investigating the photocatalysts with their particle size exceeding the UV light penetration depth. So, the 'fundamental' approach is not universal. The question of the fundamental photocatalyst activity has been challenged by Childs and Ollis [41]. They concluded that the fundamental activity is difficult to obtain and suggested to use an apparent quantum efficiency as a basis for comparison.

The 'applied' approach provides the following values for the comparison of photocatalysts: (1) the reaction rate of the unit external geometric surface area (of the photocatalyst film); (2) a quantum efficiency (the number of reaction events per photon incident on the photocatalyst); (3) a quantum yield (the number of reaction events per photon absorbed by the photocatalyst). The quantum efficiency is most often used because it is easy to evaluate.

A new advanced and still more applied type of the 'applied' approach has been proposed by Serpone et al. [42], who introduced a relative photonic efficiency as a quantum efficiency with respect to some standard photocatalytic processes. A demerit of this method is that it is impossible to compare the efficiency of significantly different processes like, for example,

[1] Photocatalytic turnover number introduced in [41] has not been taken into consideration because nowadays this value cannot be determined experimentally.

photodegradation of phenol in a gas and in a liquid phase. In this paper we compare photocatalysts on the basis of the quantum yield and the quantum efficiency.

2. Experimental

2.1. Preparation of TiO_2 photocatalysts

Specimen 1 is TiO_2 Hombikat UV 100 (anatase 100%, specific surface area 340 m^2/g), which was a kind gift from Sachtleben Chemie GmbH.

Specimen 2 is photoplatinized specimen 1. Aqueous suspension of TiO_2 after ultrasonic agitation was mixed with H_2PtCl_6 in HCl to result in 17 g/l TiO_2, $4 \cdot 10^{-4}$ M H_2PtCl_6 and pH about 1.5. The resultant mixture was irradiated by UV light for 1.5 h under continuous stirring. Theoretical Pt content is 0.4 mass.%.

Specimen 3 was prepared by thermal decomposition in air of $TiOSO_4 \cdot 2H_2O$ at 750°C for 1 h. Anatase content 100%, specific surface area 36 m^2/g.

Specimen 4 was prepared by hydrolysis of $TiOSO_4 \cdot 2H_2O$ and subsequent temperature treatment of the resultant powder at 500°C.

2.2. Reactors

Three different types of photocatalytic reactors were involved in investigation.

2.2.1. Static system

The static system used comprises a closed plexiglas 190 dm^3 chamber with a photoreactor inside the chamber. The chamber has a sampling port with a rubber septum that was used for injecting VOCs and taking samples for analysis. The scheme of the reactor is depicted in Fig. 1. Cordierite honeycomb supports were coated with TiO_2 No. 1 through depositing and drying its aqueous suspension. A fun inside the reactor blows air through the honeycomb supports illuminated by a UV middle pressure 250 W Hg lamp. The air flow through the reactor was more than 3 m^3/h providing good stirring the gas phase in the chamber.

2.2.2. Annular flow reactor

A section of this reactor is represented in Fig. 2. It includes a low pressure 15 W Hg lamp, inner and outer

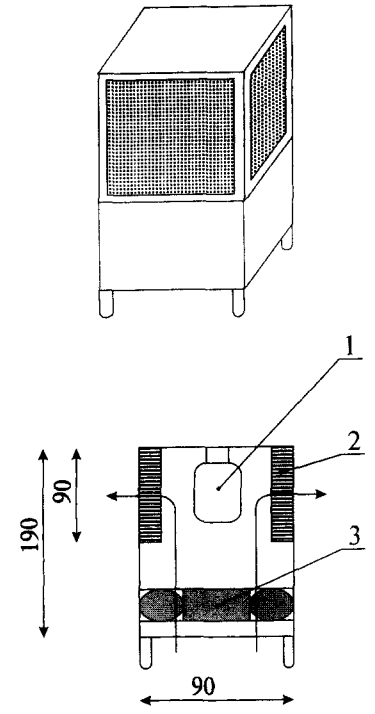

Fig. 1. Appearance and a section of the reactor used in the static system. 1 – UV lamp; 2 – honeycomb supports with deposited TiO_2; 3 – fun. The sizes are given in millimeter.

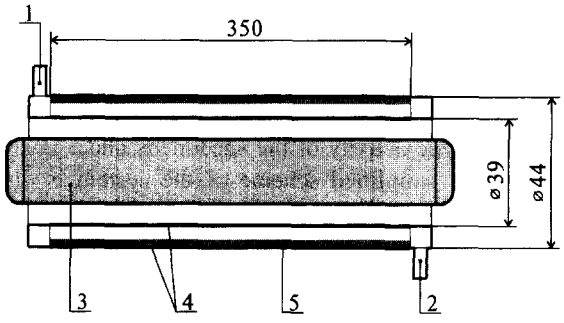

Fig. 2. A longitudinal section of the annular flow reactor. 1 – gas inlet; 2 – gas outlet; 3 – UV lamp; 4 – quartz tubes; 5 – deposited TiO_2. The sizes are given in millimeter.

quartz tubes, all these parts being arranged coaxially. TiO_2 No. 1 was loaded onto the internal surface of the outer quartz tube by applying and drying its aqueous suspension. The mass of the photocatalyst loaded was about 0.5 g resulting in the film of a thickness enough to absorb the most of the incident UV light. The flow

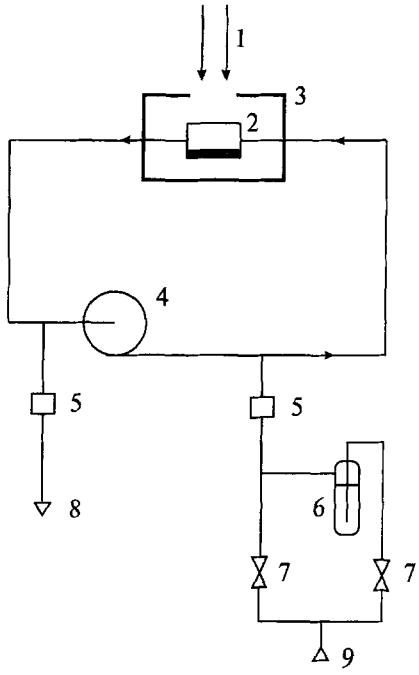

Fig. 3. A simplified drawing of the flow-circulating system used. 1 – light flux; 2 – quartz reactor; 3 – controlled temperature box; 4 – circulating pump; 5 – sampling ports; 6 – saturator with liquid VOC; 7 – air flow controllers; 8 – gas outlet; 9 – gas inlet.

of contaminated air passes between the inner and the outer quartz tubes.

2.2.3. *Flow-circulating system*

This system was used for measurements of the photocatalytic activity of the specimens under investigation. A simplified scheme of the system is displayed in Fig. 3. Two special lighting devices were used. One of them was equipped with a 1000 W high pressure Hg lamp to supply a high light intensity, and the other was equipped with a 1000 W Xe lamp and 318 nm interference filter to supply a low light intensity. Purified air passes through a saturator filled with liquid VOC and is diluted by air to adjust the VOC concentration. The same method of the air preparation was applied to feed the annular flow reactor, too. Then the air enters the flow-circulating loop consisting of a quartz reactor placed into a controlled temperature box, a circulating membrane pump and stainless steel connecting pipes. The pump provides the reaction mixture recirculation rate of approximately 5 dm^3/min that is nearly 100 times greater than the input flow rate. Hence, in this situation the conversion per pass is sufficiently low and the reactor can be considered as an ideal mixing reactor. The photocatalysts were deposited on glass plates through smearing with the aqueous suspension and drying. After this, the plates were placed into the quartz reactor. Registration of the reaction rates was carried out only after a steady-state regime had been achieved.

2.3. *Analysis*

The reactions of gaseous products were identified by means of gas chromatography, proton magnetic resonance and gas chromatography–mass spectrometry.

Concentrations of the reactants and the products were measured using gas chromatographs equipped with flame ionization and thermoconductivity detectors.

2.4. *Calculation of the quantum yields and the quantum efficiencies*

To calculate the quantum characteristics of the photocatalytic processes we assume that two UV photons are required to form each oxidizing oxygen atom. Therefore 2, 10, 16 and 24 UV photons are necessary to completely photooxidize CO, acetaldehyde, acetone and diethyl ether, respectively. This approach to the number of photons for the oxidation has also been used in [23,25,27].

To calculate the quantum yield of a photoprocess it is necessary to know the absorption rate of UV photons. Represented in Fig. 4 are diffusion reflectance spectra of thick opaque films of the photocatalysts used. Nearly all the incident photons are seen to be absorbed by the photocatalysts when the wavelength is less than 350 nm. Therefore it is easy to calculate the quantum yield when illuminating with light having wavelength less than 350 nm.

In the case of the static system it was possible only to roughly estimate the quantum efficiency due to difficulties in measuring the flux of photons incident. The latter value was estimated taking into account that the electrical power of the mercury bulb in the reactor was 38 W and assuming 20% of the electrical power to be emitted as UV light [43] half of which strikes the photocatalyst giving $1.2 \cdot 10^{-5}$ E/s.

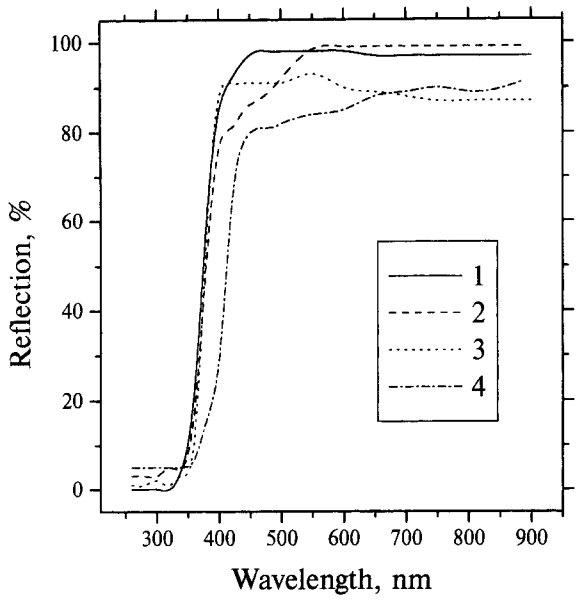

Fig. 4. Diffusion reflectance spectra of the photocatalysts studied. The reflectance of reference MgO was assumed to be 93%. The numbers correspond to the notations of the photocatalysts.

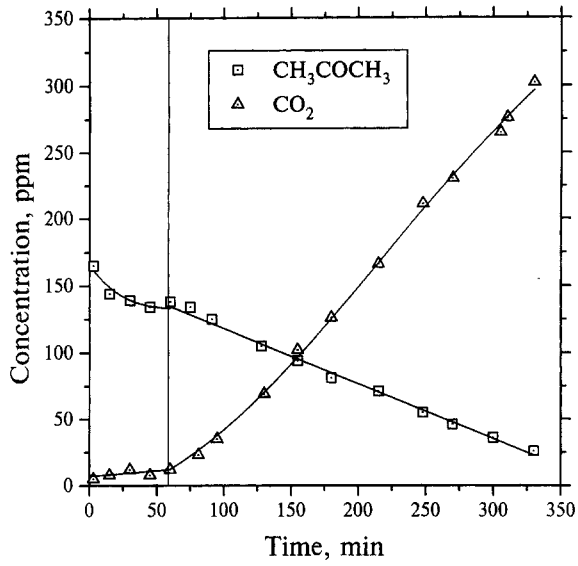

Fig. 5. Time profiles of the acetone and CO_2 concentrations in the photooxidation of acetone in the static system. Acetone was injected at t=0, the UV lamp was switched on at t=60 min.

The number of photons incident on the photocatalyst in the annular flow reactor was estimated in a similar manner giving $1.1 \cdot 10^{-5}$ E/s.

UV light intensity measurements in the reactor incorporated in the flow-circulating system were carried out for the high light intensity by an actinometrically calibrated thermoelement using light filters; for the low light intensity we used the standard ferrioxalate actinometry [44]. The values obtained are 220 and 6.9 mW/cm^2 for the unfiltered light of the 1000 W Hg lamp and for the 318 nm filtered light of the 1000 W Xe lamp, respectively.

3. Results and discussion

3.1. *Oxidation of acetone, ethanol and diethyl ether in the static system*

When oxidizing acetone, carbon dioxide appears to be the only detected gaseous product. The observed changes in the acetone and CO_2 concentrations during the acetone photooxidation are displayed in Fig. 5. Prior to commencing the illumination, the conditions in the chamber were ambient. The initial decay of the acetone concentration should be associated with its adsorption on the support and the photocatalyst. After switching on the UV lamp of the reactor, the oxidation started. A typical increase of temperature inside the chamber due to the UV lamp heating was 5°C. A small increase in the acetone concentration at the beginning of the illumination should be explained by thermal desorption. After achieving a steady temperature, the decay of the acetone concentration was linear with time and the increase of the CO_2 concentration was linear too, except for the first period when the surface intermediates of the reaction were being accumulated and the steady reaction rate was establishing. This behavior seems to result from a high coverage of the TiO_2 surface with acetone over the concentration range shown in Fig. 5. The reaction observed can be considered to proceed in agreement with stoichiometry of the following equation:

$$CH_3COCH_3 + 4O_2 \xrightarrow{16h\nu} 3CO_2 + 3H_2O \quad (1)$$

The quantum efficiency of the complete acetone oxidation was calculated from the mean rate of CO_2 evolution and estimated as 9%.

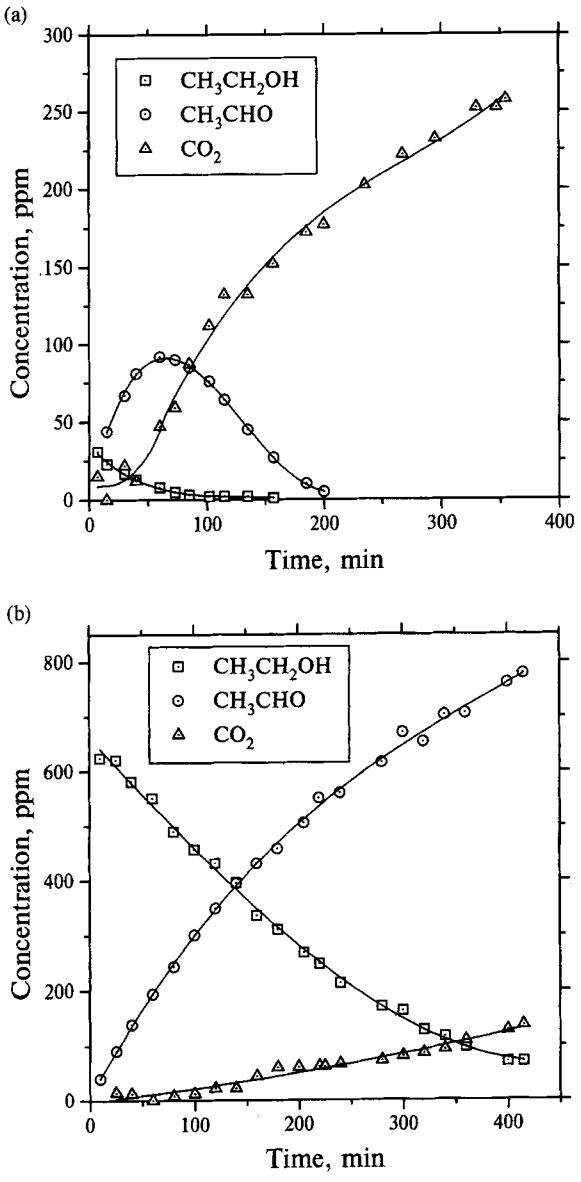

Fig. 6. Time profiles of the ethanol, acetaldehyde and CO_2 concentrations in the photooxidation of 0.1 ml (a) and 0.5 ml (b) of ethanol in the static system.

In the photocatalytic oxidation of ethanol, acetaldehyde has been identified as an intermediate gaseous product while CO_2 has been detected as the ultimate product. The concentrations of ethanol, acetaldehyde and CO_2 are plotted in Fig. 6(a) as a function of the illumination time in the oxidation of 0.1 ml of ethanol. After injection in the chamber, ethanol adsorbs quickly on the photocatalyst and supports, and only a small fraction of the injected ethanol rests in the gas phase. Without the adsorption, the ethanol concentration would be 217 ppm at the beginning of the experiment. The time behavior of the detected concentration of acetaldehyde in the chamber's air has a profile of a typical intermediate product. Thus, the ethanol oxidation is likely to proceed via two consequent reactions – oxidation of ethanol to acetaldehyde:

$$CH_3CH_2OH + \tfrac{1}{2}O_2 \xrightarrow{2h\nu} CH_3CHO + H_2O \quad (2)$$

and further complete oxidation of acetaldehyde to CO_2:

$$CH_3CHO + \tfrac{5}{2}O_2 \xrightarrow{10h\nu} 2CO_2 + 2H_2O \quad (3)$$

The increase in the CO_2 concentration after the complete depletion of gaseous ethanol and acetaldehyde is to be assigned to oxidation of the residual surface intermediates as well as to oxidation of ethanol and acetaldehyde desorbing from the unilluminated surfaces and adsorbing on the illuminated layers of TiO_2.

Reactions (2) and (3) are in competition as can be revealed by comparing Fig. 6(a) and (b). When a large ethanol quantity as 0.5 ml was being oxidized (Fig. 6(b)), reaction (2) was competing successfully with reaction (3) and only small amounts of acetaldehyde were being oxidized further to CO_2. The linear decay of the ethanol concentration likely to originate from a high TiO_2 surface coverage with ethanol extended to approximately 200 min of the irradiation. Ethanol shows stronger adsorption than acetaldehyde does. This is in agreement with data reported in [14] for oxidation of ethanol on TiO_2-loaded honeycomb support in a recirculation system, though some results of the work quoted can hardly be considered as self-consistent. The quantum efficiencies of the oxidation of ethanol to acetaldehyde according to Eq. (2) are 4% and 9% for 0.1 ml and 0.5 ml of ethanol, respectively, as calculated from the average acetaldehyde and CO_2 formation rates during first 60 min of the experiments. The quantum efficiency of the overall deep oxidation to CO_2 of 0.1 ml of ethanol approximates 9%, as calculated from the average rate of the CO_2 evolution. The fact that the quantum efficiency of the ethanol to acetaldehyde oxidation in oxidation of 0.1 ml of ethanol is less than the quantum efficiency of the complete

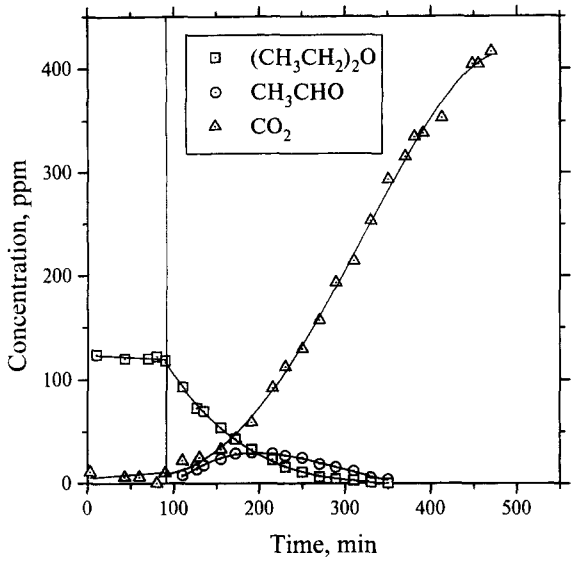

Fig. 7. Time profiles of the diethyl ether, acetaldehyde and CO_2 concentrations in the photooxidation of diethyl ether in the static system. 0.1 ml of diethyl ether was injected at t=0, the UV lamp was switched on at t=85 min.

ethanol oxidation probably reflects the uncomplete liberation of acetaldehyde into the gas phase before its further oxidation. This is in agreement with observations of Muggli et al. [45] that photocatalytic oxidation of less-than-saturation coverage of TiO_2 with ethanol does not produce gas-phase acetaldehyde.

Carbon dioxide, acetaldehyde and ethyl acetate were registered as the gaseous products of the photocatalytic oxidation of diethyl ether. Fig. 7 shows the time variation of the diethyl ether, acetaldehyde and CO_2 concentrations in the photooxidation of 0.1 ml of diethyl ether. After the injection of diethyl ether into the chamber, the ether was allowed to be adsorbed on the photocatalyst and support for 85 min with the fan on. However, only a negligible quantity of the ether was adsorbed; thus, almost all the amount of the ether injected rested in the gas phase to result in 122 ppm concentration. After the UV lamp was on, the diethyl ether concentration fell to nearly 0 in 200 min; that was accompanied by bell-shaped time profiles of the concentrations of acetaldehyde and ethyl acetate. The latter gaseous intermediate was at its top concentration of some 4 ppm at 190 min of the irradiation. The growth in the CO_2 concentration after the consumption of the gaseous organics suggests that some surface intermediates are formed during the diethyl ether oxidation as well.

The quantum efficiency of the deep diethyl ether photooxidation according to the equation

$$(C_2H_5)_2O + 6O_2 \xrightarrow{24h\nu} 4CO_2 + 5H_2O \quad (4)$$

was calculated from the average rate of CO_2 evolution and approximated 9%.

To sum up, the quantum efficiencies of as different processes as the acetone deep oxidation and the ethanol to acetaldehyde oxidation under high coverages of TiO_2 surface with organics appear to be close to 9%. Though the light intensity estimation was rough, all the quantum efficiencies were calculated on the common basis allowing to make their relative comparison. Assuming that the number of active sites for the above two processes is the same, one can deduce that the nature of the adsorbed organic compound does not influence the quantum efficiency of its oxidation. Thus, this efficiency may be defined mostly by production of an active oxidizing oxygen, as it was concluded in [1] considering the correlation between the photocatalytic activity for the gas–solid oxygen isotope exchange and for the CO and ethane oxidation on a number of TiO_2 specimens.

It is easy to determine that the volume of air equivalent to that of the chamber passes through the reactor in 3.8 min. Typical times of the complete conversion of the organics under study were 200 min or more. Therefore, the conversion per pass was less than 2%. No doubt that this low value results from a short residence time of VOCs in the honeycomb supports, which is estimated as 0.2 s.

3.2. *Oxidation of acetone in the annular flow reactor*

The annular flow reactor used allowed to use low air flow rates and consequently to obtain long residence times. Therefore, high conversions per pass might be expected to occur. Some experimental results of the acetone oxidation are presented in Table 1. It is seen that the almost complete acetone conversion is achievable in this reactor at the flow rates up to ca. 0.5 dm^3/min and at the inlet acetone concentration ca. 500 ppm. The concentration of CO_2 evolved was in

Table 1
Some data on the photocatalytic oxidation of acetone in the annular flow reactor

Gas flow (dm^3/min)	Residence time (min)	Acetone inlet concentration (ppm)	Acetone conversion (%)	Quantum efficiency (%)
0.11	4.1	554	99.6	5.5
0.18	2.5	520	99.9	8.4
0.32	1.4	460	99.9	14
0.54	0.84	470	99.9	23
1.2	0.38	466	63	32

agreement, within the experimental error, with acetone concentration converted according to Eq. (1); this suggests that the acetone was oxidized rather than consumed by the adsorption on the photocatalyst. The quantum efficiency of the acetone photooxidation increased with a growth in the flow rate as a result of increasing the average acetone concentration throughout the reactor.

3.3. *Acetone oxidation in the flow-circulating reactor*

3.3.1. *Comparison of the photocatalysts activity*

Since acetone does not form any detectable gaseous intermediates when being photooxidized, the rate of its complete oxidation to CO_2 is easy to control. Because of this reason, acetone has been chosen as a test substance for comparison of the photocatalysts activity.

It has been concluded in the experimental, from the diffusion reflectance spectra of the photocatalysts studied, that the quantum efficiency becomes in fact quantum yield when illuminated with light having wavelength less than 350 nm. So, the photocatalytic activity of the specimens is given here as the quantum yield when 318 nm filtered light is used.

The quantum efficiencies of the reaction over the catalyst specimens under the high intensity UV light are depicted in Fig. 8(a). Shown in Fig. 8(b) are the quantum yields of the reaction on all the specimens studied under the low intensity 318 nm filtered light. It is seen in these diagrams that though specimen 1 seems to be the most active one, the other specimens are also sufficiently active. The facts show that the illumination of the photocatalysts with the high intensity light of the Hg lamp leads to the lower quantum efficiencies than illumination with the low intensity 318 nm filtered light of the Xe lamp which can be attributed either to detrimental effect of higher light intensity [46], or to different spectra of these two light sources, or to an effect of light pulsation (the Hg lamp used is fed by 50 Hz AC contrasting with the DC fed Xe lamp used). Unexpectedly, it has been found that platinization of specimen 1 resulting in specimen 2 provides a negative effect on the photocatalytic activity. In the literature, an opposite effect has been reported for the case when platinization has been carried out by reduction of H_2PtCl_6 with $NaBH_4$ [12]. Therefore, the observed retardation of the photocatalytic oxidation may arise from the platinization method used.

It has been reported in [47] that photocatalytic platinization of TiO_2 proceeds through the conversion of hydrolyzates of $PtCl_6^{2-}$ and stops at pH<2–3. Although we carried out the platinization at pH about 1.5, there are some evidences of Pt deposition, viz. the characteristic change in the diffusion reflectance spectrum and a high activity in the CO photocatalytic oxidation reported below.

3.3.2. *Temperature dependence of the photocatalytic activity*

Fu et al. [12] have reported that the rate of photooxidation of gaseous benzene increases with temperature in the range 70–140°C. So, of interest is also the temperature dependence of the acetone photooxidation. The recorded change in the reaction quantum efficiency with temperature in the limits of 40–163°C is represented in Fig. 9(a). The quantum efficiency calculated from the CO_2 concentration appeared due to the complete photooxidation of acetone. One can see that the quantum efficiency increases until temperature reaches 80°C and then it decreases. No evolution of CO_2 has been detected when

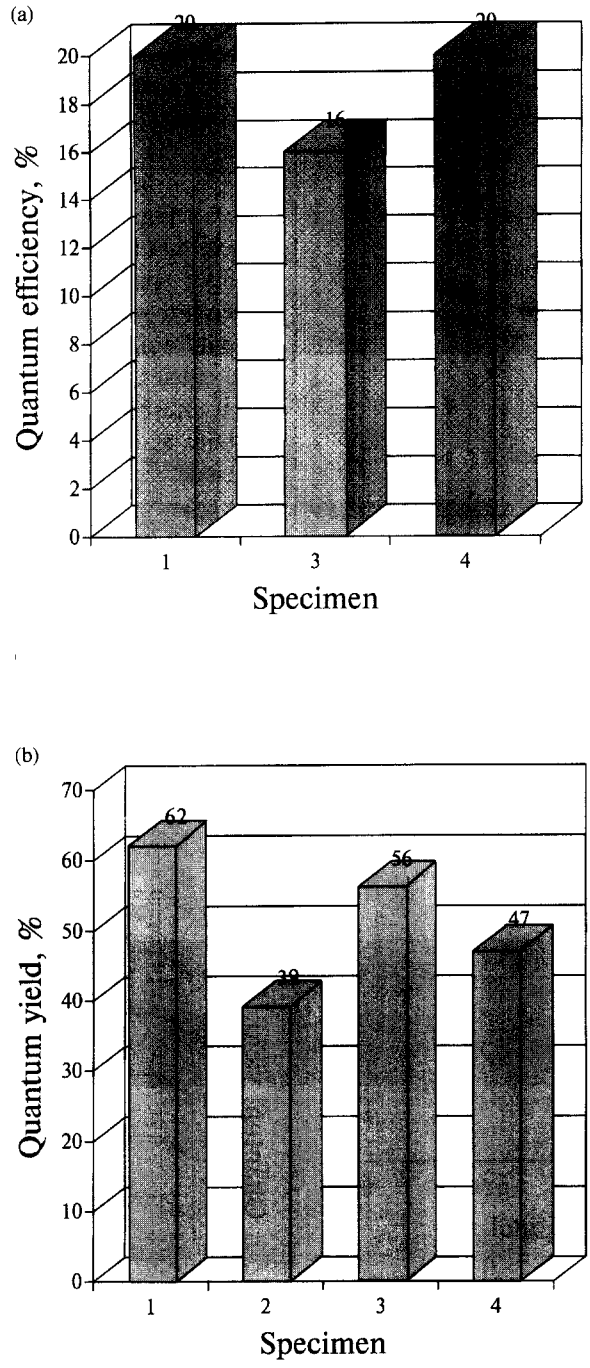

Fig. 8. Diagram of the photocatalytic activity of the studied TiO_2 specimens in the flow-circulation system under (a) high light intensity of 220 mW/cm^2 and (b) low light intensity of 6.9 mW/cm^2. Acetone concentration 500 ppm, temperature 40°C.

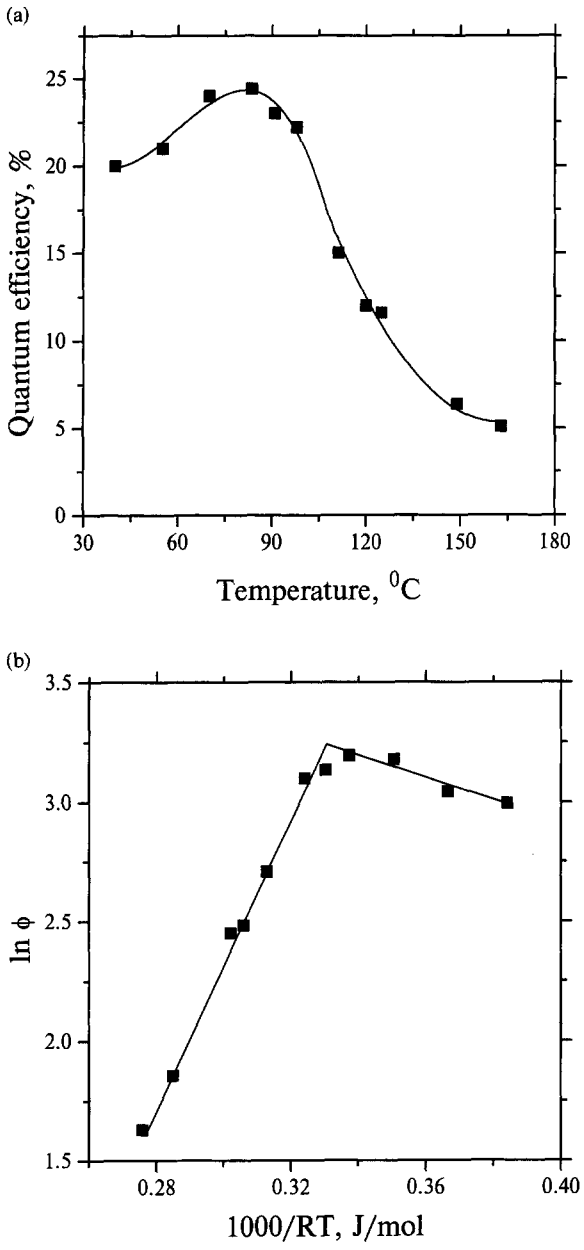

Fig. 9. Quantum efficiency, ϕ, of the complete photooxidation of acetone over specimen 4 as a function of temperature (a) and the apparent Arrhenius plot of this process (b). Acetone concentration 500 ppm, UV light intensity 220 mW/cm^2.

an attempt was undertaken to oxidize acetone in the dark either at 74°C or at 149°C. The apparent activation energies obtained from the Arrhenius plot in Fig. 9(b) are 4.7 kJ/mol for the ascending section and −29 kJ/mol for the descending section of the temperature dependence.

A variation of the photocatalyst color with temperature has also been observed. After the operation at 120°C, the color was yellow, after the operation at 163°C, it became brown. A dark coloration of TiO_2 after being used at higher temperatures was also reported in [12]. The initial white color of our photocatalyst appeared to be almost completely restored when it then operated at 72°C for 1.5 h. Though, the activity was not completely recovered and the quantum efficiency at 72°C was only 16% instead of 24% for the fresh photocatalyst. Consequently, a drop of the activity at temperatures in excess of 80°C can be ascribed, at least partially, to deactivation processes.

3.4. *Carbon monoxide photooxidation in the flow-circulating reactor*

Some information available in literature [40] contains assertion that titanium dioxide can considerably differ in activity toward the CO photooxidation depending on whether it was prepared by hydrolysis

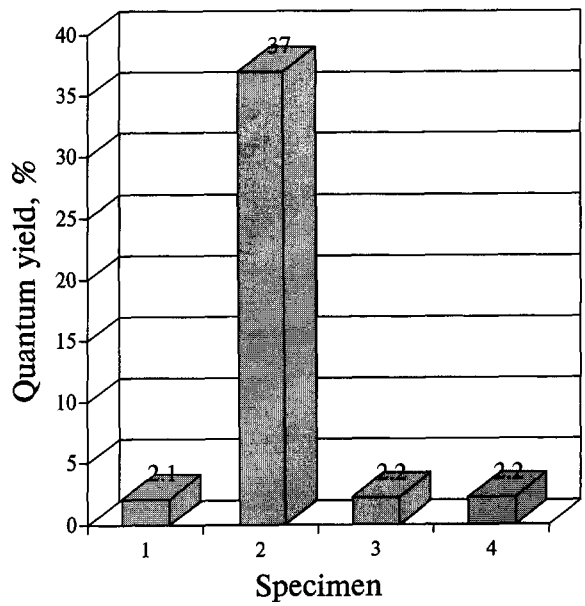

Fig. 10. Diagram of the photocatalytic activity of the studied TiO_2 specimens in CO photooxidation in the flow-circulating system. CO concentration 5000 ppm, UV light intensity 6.9 mW/cm^2, temperature 40°C.

or by thermal decomposition. By testing our specimens in the reaction, one could obtain more comprehension of how the preparation method affects the photocatalytic activity.

The results of measurements of the photocatalytic activity in the CO oxidation are plotted in Fig. 10. The oxidation has been demonstrated to stop when light was switched off. One can see that the activity was low and equal in the limits of experimental error for TiO_2 prepared by either hydrolysis in aqueous media (specimen 4) or pyrolysis (specimens 1 and 3). Note that platinization improves photoactivity appreciably.

4. Conclusion

1. When vapors of acetone, ethanol and diethyl ether are subjected to photocatalytic oxidation over TiO_2 in a reactor with a short residence time, their conversion per pass is low and intermediate gaseous products are formed: none in the acetone oxidation, acetaldehyde in the ethanol oxidation, acetaldehyde and ethyl acetate in the diethyl ether oxidation; CO_2 is the final carbon-containing product for all the mentioned substrates.
2. Complete photocatalytic oxidation of acetone was demonstrated during a single pass through the annular flow reactor having a high residence time for the acetone.
3. Specimens of TiO_2 prepared by different methods have proved to possess rather high photocatalytic activity in the oxidation of acetone; however, photoplatinization has turned out to lead to a partial deactivation of the photocatalyst for this reaction.
4. A maximum has been revealed in the temperature dependence of the rate of the acetone photooxidation; this maximum can be assigned, at least partially, to catalyst deactivation.
5. Photoplatinized TiO_2 has been shown to have an advanced activity in the photocatalytic oxidation of CO while the unplatinized specimens of TiO_2 appeared to be low active.

The above results demonstrate a high potentiality of the photocatalytic oxidation of both VOCs and CO over TiO_2 for optimization to be used in practical air purification.

References

[1] S. Sato, T. Kadowaki, J. Catal. 106 (1987) 295.
[2] N. Djeghri, M. Formenti, F. Juillet, S.J. Teichner, Faraday Disc. Chem. Soc. 58 (1974) 185.
[3] N. Djeghri, S.J. Teichner, J. Catal. 62 (1980) 99.
[4] A.V. Emelin, V.K. Ryabchuk, D. Purevdordge, G.N. Kuzmin, in: V. Krishnan (Ed.), Proceedings of the 11th International Conference on Photochem. Conv. Storage Sol. Energy (IPS-11), 1996, p. 203.
[5] M. Daroux, D. Klvana, M. Duran, M. Bideau, Can. J. Chem. Eng. 63 (1985) 668.
[6] J.M. Herrmann, J. Disdier, M.-N. Mozzanega, P. Pichat, J. Catal. 60 (1979) 369.
[7] V.N. Filimonov, Kinetika I Kataliz. 7 (1966) 512.
[8] P. Witier, L. Estaque, P.C. Roberge, S. Kaliaguine, Can. J. Chem. Eng. 55 (1977) 352.
[9] Y. Weng, F. Wang, L. Lin, R. Xie, in: D.F. Ollis, H. Al-Ekabi (Eds.), Photocatalytic Purification and Treatment of Water and Air, Elsevier, Amsterdam, 1993, p. 713.
[10] P. Pichat, J.-M. Herrmann, J. Disdier, M.-N. Mozzanega, Can. J. Chem. Eng. 60 (1982) 27.
[11] T.N. Obee, R.T. Brown, Environ. Sci. Technol. 29 (1995) 1223.
[12] X. Fu, W.A. Zeltner, M.A. Anderson, Appl. Catal. B. 6 (1995) 209.
[13] K. Suzuki, in: D.F. Ollis, H. Al-Ekabi (Eds.), Photocatalytic Purification and Treatment of Water and Air, Elsevier, Amsterdam, 1993, p. 421.
[14] M.L. Sauer, D.F. Ollis, J. Catal. 158 (1996) 570.
[15] M.L. Sauer, M.A. Hale, D.F. Ollis, J. Photochem. Photobiol. A 88 (1995) 169.
[16] J. Peral, D.F. Ollis, J. Catal. 136 (1992) 554.
[17] D.S. Muggli, S.A. Larson, J.L. Falconer, J. Phys. Chem. 100 (1996) 15886.
[18] R.I. Bickley, G. Manuera, F.S. Stone, J. Catal. 31 (1973) 398.
[19] V.N. Filimonov, Dokl. Akad. Nauk SSSR 154 (1964) 922.
[20] V.N. Filimonov, Dokl. Akad. Nauk SSSR 158 (1964) 1408.
[21] A. Walker, M. Formenti, P. Meriaudeau, S.J. Teichner, J. Catal. 50 (1977) 237.
[22] J. Cunningham, B.K. Hodnett, J. Chem. Soc. Faraday Trans. 1 77 (1981) 2777.
[23] I. Sopyan, S. Murasawa, K. Hashimoto, A. Fujishima, Chem. Lett. (1994) 723.
[24] N. Takeda, T. Torimoto, S. Sampath, S. Kuwabata, H. Yoneyama, J. Phys. Chem. 99 (1995) 9986.
[25] I. Sopyan, M. Watanabe, S. Murasawa, K. Hashimoto, A. Fujishima, J. Photochem. Photobiol. A 98 (1996) 79.
[26] M.L. Sauer, D.F. Ollis, J. Catal. 149 (1994) 81.
[27] S. Sampath, H. Uchida, H. Yoneyama, J. Catal. 149 (1994) 189.
[28] A. T-Raissi, N.Z. Muradov, in: D.F. Ollis, H. Al-Ekabi (Eds.), Photocatalytic Purification and Treatment of Water and Air, Elsevier, Amsterdam, 1993, p. 435.
[29] M.R. Nimlos, W.A. Jacoby, D.M. Blake, T. Milne, in: D.F. Ollis, H. Al-Ekabi (Eds.), Photocatalytic Purification and Treatment of Water and Air, Elsevier, Amsterdam, 1993, p. 387.

[30] W. Holden, A. Marcellino, D. Valic, A.C. Weedon, in: D.F. Ollis, H. Al-Ekabi (Eds.), Photocatalytic Purification and Treatment of Water and Air, Elsevier, Amsterdam, 1993, p. 393.
[31] M.A. Anderson, S. Yamazaki-Nishida, S. Cervera-March, in: D.F. Ollis, H. Al-Ekabi (Eds.), Photocatalytic Purification and Treatment of Water and Air, Elsevier, Amsterdam, 1993, p. 405.
[32] H. Al-Ekabi, B. Butters, D. Delany, W. Holden, T. Powell, J. Story, in: D.F. Ollis, H. Al-Ekabi (Eds.), Photocatalytic Purification and Treatment of Water and Air, Elsevier, Amsterdam, 1993, p. 719.
[33] K. Wang, B.J. Marinas, in: D.F. Ollis, H. Al-Ekabi (Eds.), Photocatalytic Purification and Treatment of Water and Air, Elsevier, Amsterdam, 1993, p. 733.
[34] L.A. Dibble, G.B. Raupp, Catal. Lett. 4 (1990) 345.
[35] M.R. Nimlos, W.A. Jacoby, D.M. Blake, T.A. Milne, Environ. Sci. Technol. 27 (1993) 732.
[36] W.A. Jacoby, M.R. Nimlos, D.M. Blake, Environ. Sci. Technol. 28 (1994) 1661.
[37] L.A. Phillips, G.B. Raupp, J. Molec. Catal. 77 (1992) 297.
[38] A. Linsebigler, G. Lu, J.T. Yates, J. Phys. Chem. 100 (1996) 6631.
[39] H. Damme, W.K. Hall, J. Catal. 69 (1981) 371.
[40] F. Juillet, F. Lecomte, H. Mozzanega, S.J. Teichner, A. Thevenet, P. Vergnon, Faraday Symp. Chem. Soc. 7 (1973) 57.
[41] L.P. Childs, D.F. Ollis, J. Catal. 66 (1980) 383.
[42] N. Serpone, G. Sauve, E. Pelizzetti, M.A. Fox, in: G. Calzaferri (Ed.), Proceedings of the 10th International Conference on Photochem. Conv. Storage Sol. Energy (IPS-10), 1994, p. 121.
[43] J.F. Rabek, Experimental Methods in Photochemistry and Photophysics, Wiley, Chichester, 1982.
[44] C.A. Parker, Photoluminescence of Solutions, Elsevier, Amsterdam, 1968.
[45] D.S. Muggli, S.A. Larson, J.L. Falconer, J. Phys. Chem. 100 (1996) 15886.
[46] T. Watanabe, A. Kitamura, E. Kojima, C. Nakayama, K. Hashimoto, A. Fujishima, in: D.F. Ollis, H. Al-Ekabi (Eds.), Photocatalytic Purification and Treatment of Water and Air, Elsevier, Amsterdam, 1993, p. 747.
[47] J. Zhensheng, X. Changjuan, L. Qinglin, C. Zhengshi, in: G. Calzaferri (Ed.), Proceedings of the 10th International Conference on Photochem. Conv. Storage Sol. Energy (IPS-10), 1994, p. 129.